PITHIA-NRF

Report 2022

THE SOCIOECONOMIC IMPACTS OF THE UPPER ATMOSPHERE EFFECTS ON LEO SATELLITES, COMMUNICATION, AND NAVIGATION SYSTEMS

ETHNIKO ASTEROSKOPEIO ATHINON (NOA)
www.noa.gr
Research Director:
Dr. Anna Belehaki | belehaki@noa.gr

The PITHIA-NRF project has received funding from the European Union's Horizon 2020 research and innovation program under grant agreement No 101007599

Contents

1. Executive Summary

The near-Earth space environment undergoes daily changes driven by variable conditions in the Sun. Explosive eruptions of energy from the Sun causing minor solar storms on Earth are relatively common and of little consequence. On the contrary, rarely occurring superstorms generate physical changes in the Earth's upper atmosphere detrimental to satellites, signals from global navigation systems, and radio systems.

While these events' physics and engineering repercussions have been studied extensively, this is not the case for the related socioeconomic ramifications, despite our growing dependence on these technologies. Therefore, the report identifies the infrastructures vulnerable to the upper atmosphere effects and quantifies their impacts on LEO satellites, systems offering PNT services, and radio systems through a systematic literature review.

In summary, we find that the costs associated with the risks posed to critical space-borne and ground-based technologies by upper atmospheric events are high, comparable to those of terrestrial hazards like tsunamis, earthquakes, or floods. Nevertheless, the quantification of the socioeconomic impacts is not yet mature, partly because of the lack of important modeling information and modern society's lack of experience with extremely large events. Nonetheless, governments, asset owners, and business managers need advances in this area to mitigate the risks posed by upper atmosphere space weather.

2. Introduction

PITHIA-NRF is a Research Infrastructure project funded by the European Commission Horizon 2020 Programme. PITHIA-NRF aims to build a distributed network that integrates into a unified research environment all key observing facilities, data collections, data processing tools, and prediction models dedicated to the ionosphere, thermosphere, and plasmasphere research. By integrating different assets, PITHIA-NRF offers R&D services to experts, early-career researchers, and software and instrument development professionals, enabling leading-edge research and fostering innovation.

PITHIA-NRF has the ambition to become the European hub that will act as a facilitator for coordinated observations, for data processing tools and modeling advances, for software and data-products standardization. It will advise on the transitioning of models to operations by providing e-science supporting tools so that models can reach the desired accuracy and standards.

Many operational systems that are critical for the quality of life and the safety of European citizens rely on the upper atmosphere for their operations. Such is the case of radio communication, HF geolocation, or broadcasting systems. Upper atmosphere disturbances can affect, or even worse, disrupt such systems. Similarly, for other types of infrastructures, the upper atmosphere represents a nuisance: this is the case for trans ionospheric radio communication and navigation systems (GNSS, EGNOS, GBAS, N-RTK, and radio astronomy observations). Thus, these infrastructures can experience essential performance degradations and become unreliable. It follows that these systems require accurate information about the current state of the upper atmosphere and the expected effects of forthcoming space weather disturbances – especially the extreme space weather, to support the long-term planning of their operations. PITHIA-NRF develops the innovation framework to support software and hardware R&D projects by implementing science and engineering solutions to help users develop relevant applications efficiently.

This report summarizes the socioeconomic effects of the upper atmosphere space weather impact, encouraging a discussion with the project stakeholders for potential collaboration within the innovation framework of the PITHIA-NRF project.

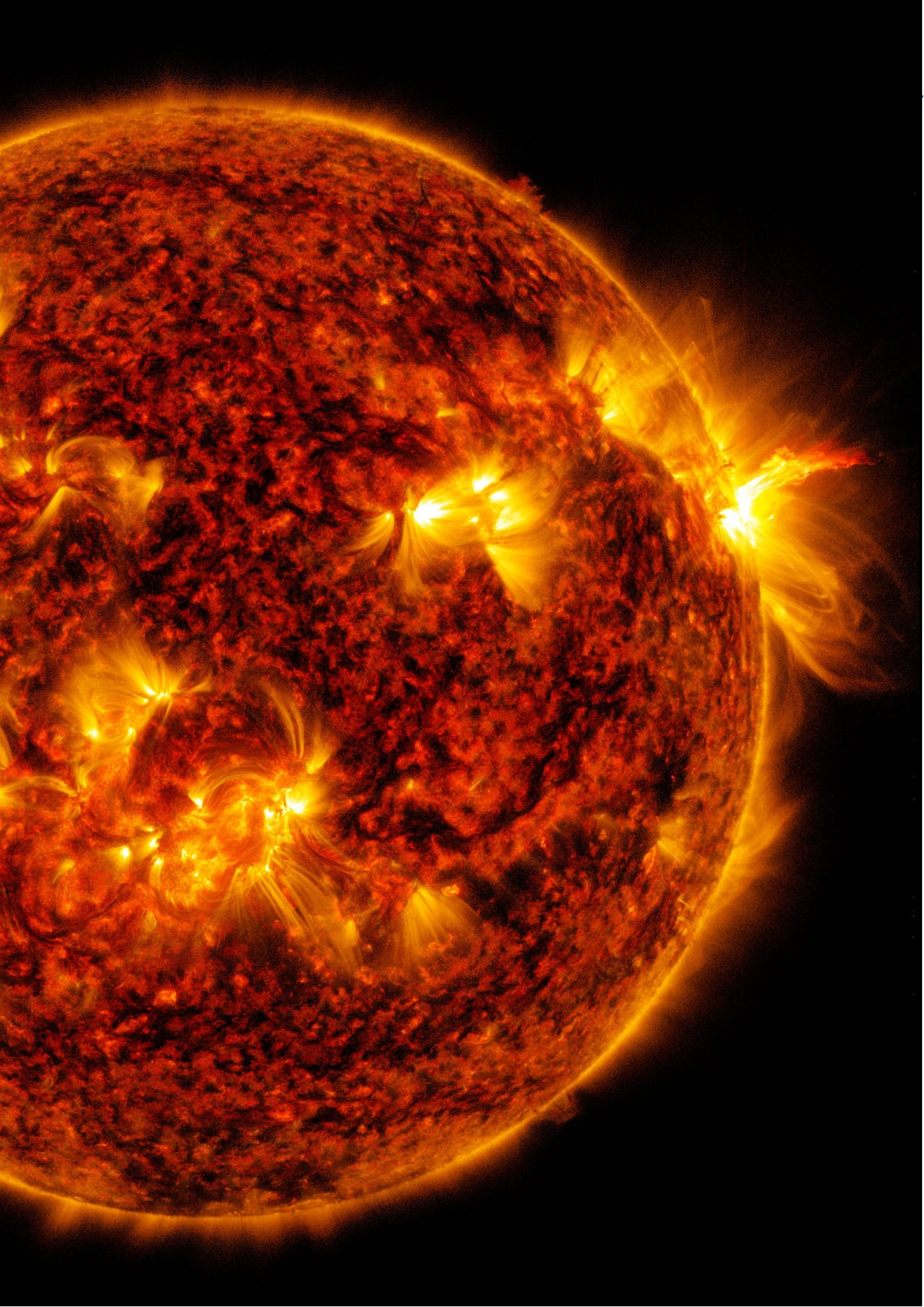

3. Phenomena with potential impacts

This report presents a systematic literature review undertaken ad hoc to describe the effects and quantify the related impact of upper atmosphere space weather, i.e., those variations in the Sun, ionosphere, and thermosphere, influencing space-borne and ground-based technological systems' performance and reliability (Cannon, 2013).

Specifically, the report focuses on the ionosphere's impacts on radio and navigation systems and thermospheric effects on satellites in low-Earth orbit (LEO) (Figure 1).

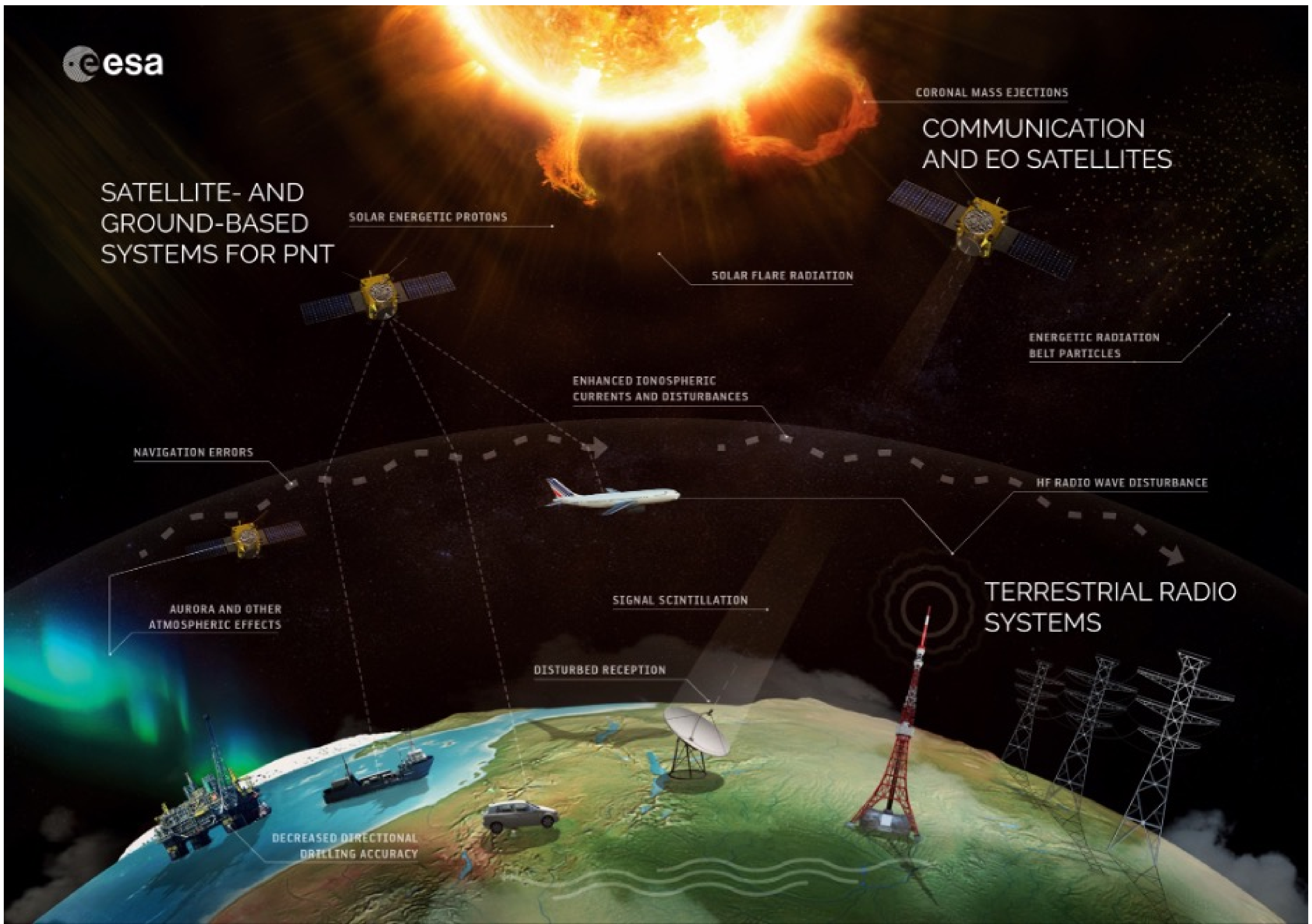

Figure 1. Schematic representation of the upper atmosphere space weather effects on space- and ground-based infrastructures (adapted from ESA's "Space Weather Effects" image, retrieved at https://www.esa.int/ESA_Multimedia/Images/2018/01/Space_weather_effects on April 11, 2022).

The ionosphere is a lightly ionized region of the upper atmosphere that extends from about 60 to 2,000 km above the Earth, with a density peak at around 300km altitude. It is conventionally divided into four latitudinal regions: equatorial, mid-latitude, auroral, and polar cap.
One of the reasons for which the ionosphere is essential to, e.g., radio communications systems, is that the ionospheric plasma is conductive and, therefore, interacts with electromagnetic waves.

However, the ionospheric plasma is highly variable over space and time, with spatial scales ranging from thousands of kilometers to less than a meter and temporal scales ranging from many years to hours or even minutes and seconds (Cander, 2019). Due to phenomena originating below (meteorological events, earthquakes, explosions) or coming from above (space weather events), such high variability poses complex challenges to radiocommunications and navigation systems operators that need reliable models for forecasting and nowcasting ionospheric conditions.
As illustrated in Figure 2, the ionosphere consists of three main regions: the D-region, the E-region, and the F-region, each playing a different role in radio propagation.

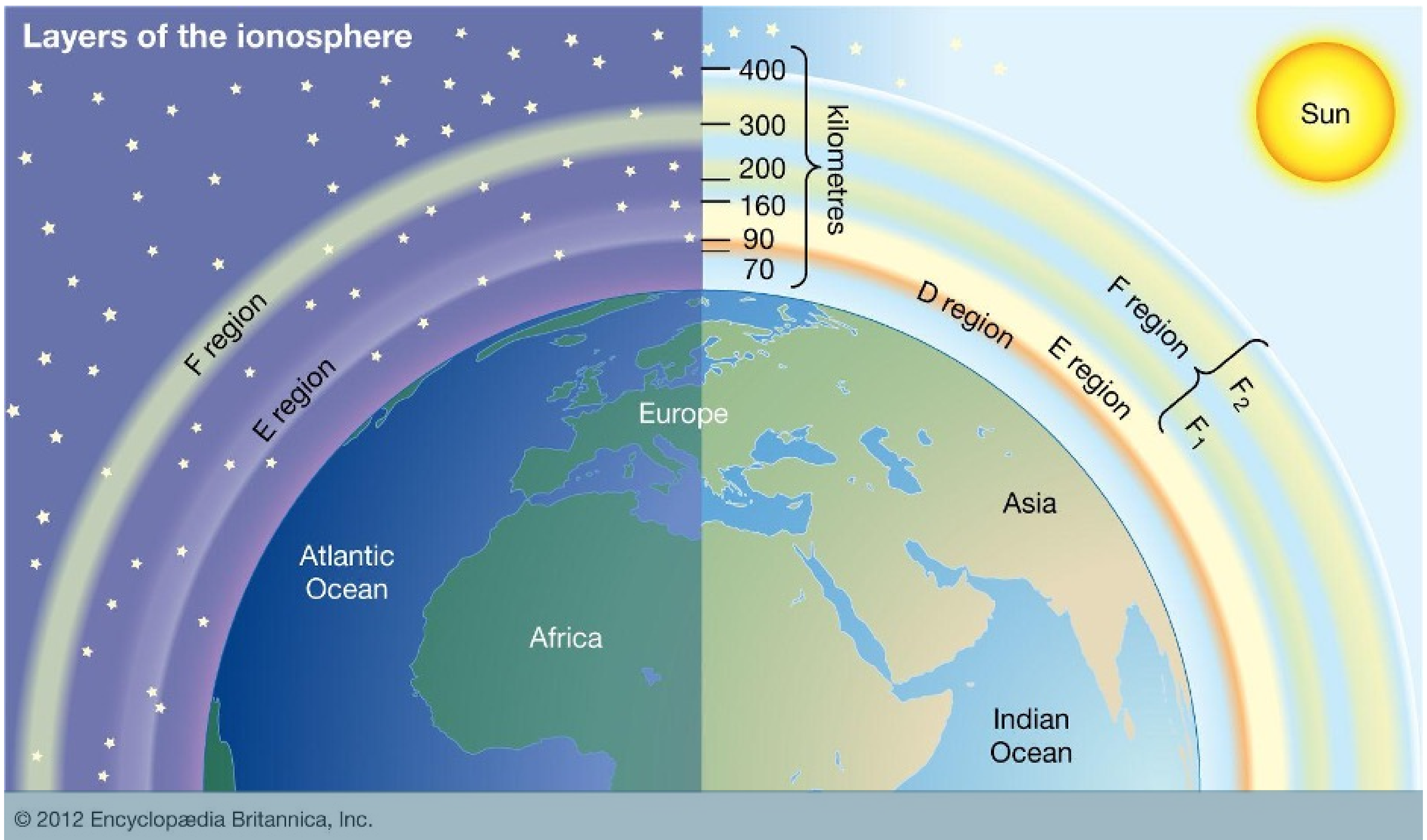

Figure 2. Layers of the Earth’s ionosphere (retrieved from Encyclopædia Britannica at https://www.britannica.com/science/D-region#/media/1/149302/167048 on April 11, 2022)

The F region is the most variable and complex ionospheric layer, presenting the highest density of free electrons and positively charged ions. Its fundamental importance for radio communication follows from these properties:

1. It is present 24 h a day even though weak in the early morning hours;
2. Its high altitude allows the longest communication paths;
3. It usually reflects the high-frequency (HF) electromagnetic waves with less absorption and the highest bit rate.

Therefore, most of all HF communication links are planned, assuming the exploitation of the F region, in the highly populated mid-latitudes (Cander, 2019).

Under quiet conditions, the ionosphere enables radio communications possible. At the same time, it represents the primary source of inaccuracy for global navigation satellite systems (GNSS) and the second source for differential GNSS (Section 2). The GNSS signal is transmitted by satellites flying at about 20,000 km that are received on the ground by GNSS receivers. The presence and the distribution of free electrons in the ionosphere modify the traveling GNSS signal's phase and amplitude, inducing degradation in the navigation service.

In general, the space weather sources of upper atmosphere phenomena listed in Table 1 affecting radio and navigation systems are

A. Geomagnetic storms, i.e., disturbances in the geomagnetic field caused by gusts of solar wind moving past the Earth;

B. Solar radiation storms, i.e., high levels of radiation that occur when the numbers of energetic particles increase;

C. Solar flares, i.e., X-rays emissions from the Sun.

Geomagnetic storms are also the primary source of uncertainty in the position of all objects in LEO, especially satellites, which fly into the thermosphere (the neutral counterpart of the ionosphere). As the thermosphere experiences strong variation in the neutral density due to radiative inputs from the Sun in the extreme ultraviolet wavelength range, energetic particles precipitation in the auroral zones, and global‐scale electrical currents generated during geomagnetic storms, drag forces start acting on satellites flying through the thermosphere, causing orbital track changes (Berger et al., 2020).

Source [Propagation time from Sun to Earth]	Provisional indicators	Upper atmosphere phenomena
Electromagnetic radiation [8 min]	Short- and long-term variability of Solar radio indices F10.7, F30	SIDS
	Level of radio noise in selected frequency bands (e.g., the L-band)	SIDS
	Perturbation in the electron density profile	SIDS; Spread F; TIDS.
ICME and HSS [13 hrs to 4 days]	IMF characteristics at L1 Lagrangian point	Geomagnetic storms & auroral electrojet intensification; Plasma bubbles; TIDS; Scintillations.
	AE index	Auroral electrojets intensification
	Dst index	Ring current enhancement
	Kp index	Magnetospheric electric current systems
	Ionospheric bottom side characteristics and TEC; TEC gradients	Geomagnetic storms & auroral electrojet intensification; Plasma bubbles; TIDS; Scintillations
	Doppler shift Electron density gradients	TIDS
	TEC depletions	Plasma bubbles
High SEP [~ 1 hr]	D-region absorption	PCA
ICME, CH, Particle precipitation, penetrating electric fields [unknown]	Scintillation indices and ROTI	Scintillations

Table 1. Summary of the upper atmosphere phenomena relevant to this report. The scientific background for this table is covered in the Glossary.

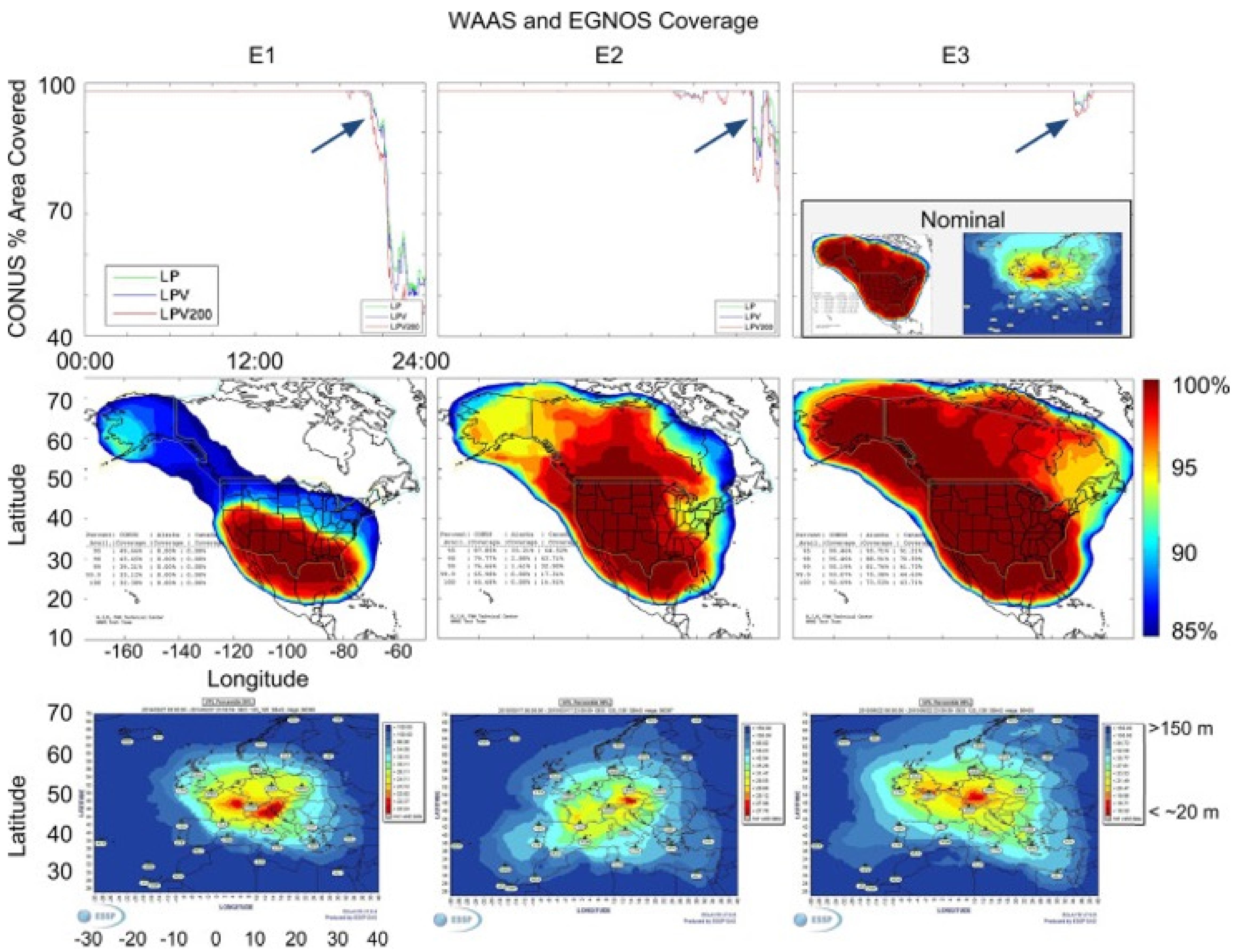

Figure 3. North America WAAS and European EGNOS aviation systems impacts for the events happened on, from left to right, February 27, 2014, March 17, 2015, and June 22, 2015 (Redmon et al., 2018)

" St. Patrick's Day" event, a geomagnetic superstorm from last solar cycle

RECENT EXAMPLES

July 15, 2000 - A CME-driven storm caused the total loss of the LEO satellite Astro-D (ASCA) due to thermospheric drag (Cannon, 2013).

December 6, 2006 - The largest solar radio burst ever recorded affected GPS receivers over the entire sunlit side of the Earth. There was a widespread loss of GPS in the mountain states region, specifically around the four corners region of New Mexico and Colorado. Additionally, several aircraft reported losing lock on GPS.

August 9, 2011 - A major solar flare caused fade-outs in the SW broadcasts of Radio Netherlands World for an hour.

January 23, 2012 - An M9-class solar flare disrupted broadcasts on the 6 - 20 meters bands across North America and severely affected the UHF and VHF bands for a few hours.

February 27, 2014 - A relatively modest geomagnetic storm (minimum Disturbance Storm-Index (Dstmin)≈ − 94 nT) degraded the performance of the US Wide Area Augmentation System (WAAS) navigation service covering eastern Alaska and the north-eastern continental United States, and the similar European Geostationary Navigation Overlay Service (EGNOS) covering northern Europe

March 17, 2015 [June 22, 2015] - The “St. Patrick's Day” event (Dstmin ≈ − 223 nT [Dstmin ≈ − 204 nT]) resulted in the most intense geomagnetic storm of the last solar cycle, with mid-latitude auroral sightings and severe ionospheric irregularities. Both events impacted WAAS and EGNOS services over important coverage areas (Figure 3).

Did you know?

Government agencies, satellite and other space asset operators and designers, and power grid operators use the Disturbance Storm Time (Dst) index to analyze the strength and duration of geomagnetic storms. Dst is a measure of the decrease in the horizontal component of the Earth’s magnetic field near the magnetic equator due to increases in the magnetospheric ring current (see the FAQ below). Values less than −50 nanotesla (nT) indicate high geomagnetic activity. The "Carrington event" generated the strongest registered geomagnetic storm with Dst ≈ −1700 nT (page 24, Table 3)!

The original Dst index is provided by the World Data Center for Geomagnetism, Kyoto, Japan.

4. Impacted systems and services

Space-borne Infrastructures

EARTH OBSERVATION (EO) SATELLITES IN LEO

The Earth and its surroundings are continuously monitored by multiple satellites. These spacecraft offer information about the dynamic state of the Earth's environment and its surroundings by providing regular and frequent observation of geophysical parameters.

Remote sensing systems convey invaluable data on the Earth's climate and weather (e.g., temperature, cloud cover), ground biomass change, land cover types, the state of the oceans' surface and currents, and enable the development of high-resolution topographic maps. Some satellites also observe the upper layers of the atmosphere and the exosphere measuring the fluctuations of the magnetic field and of energetic particles flux. In addition, the spacecraft monitoring the Sun and the solar wind are used in issuing space weather alerts to prepare the users for imminent solar storms.

However, operating in frequencies from high-frequency (HF, 3-30 MHz frequency range, 100 to 10 m spatial range) to ultra HF (UHF, 300 - 3000 Mhz frequency range, 1 m to 1 dm spatial range), EO systems are vulnerable to upper atmosphere phenomena (UAP). For instance, ionospheric scintillations and TEC gradients can corrupt images created by space-based synthetic aperture radars (SARs), like ESA's P-band (435 MHz) Biomass SAR, which operates in LEO (Alfonsi et al., 2018).

In the short term, interruptions to remote sensing would degrade weather broadcasting or hinder disaster response and relief (by reducing the quality of real-time maps). Furthermore, in a worst-case scenario, such as the loss of EO satellites from thermospheric drag, the long-term ability to run global climate and ecosystemic models that rely on EO data would be jeopardized.

Impacted systems	SPACE-BASED SYSTEMS		GROUND-BASED SYSTEMS		
Impacted services	LEO cellular and data SATCOM VLF-MF communications and broadcasting	EO (with LEO satellites), Space-based SAR	PNT with GNSS and GBAS	Astronomical observation systems (LOFAR)	Terrestrial radio systems (HF communications)
Impacting UAP	Ionospheric plasma bubbles; Multipath Attenuation Doppler	Faraday Rotation; Ionospheric Scintillation; Atmospheric drag	Large TEC gradients; Ionospheric plasma bubbles (leading to scintillations and ionospheric delays); TIDS	Geomagnetic storms; Auroral jets intensification; Ionospheric plasma bubbles	PCA; Sporadic E-layer; TIDS; Ionization depletions
Effects	Rapid fluctuations in the amplitude and phase of the radio signal leading to repeated disruption of communications links	Loss of phase coherence across SAR aperture Prohibits remote sensing	Loss of phase lock and data loss Range errors	Radio signal refraction	Blackout of HF radio frequencies
Worst-case scenario duration and spatial extent of effects	Intermittent occurrence over several days worldwide	SAR: 1 hour on the whole dayside of the Earth EO: asset loss	Intermittent occurrence over several days worldwide		Two or three hours in all regions at low- and mid-latitude on the dayside of the Earth (solar flare) Several days at high latitudes (PCA)

Table 2. Summary of the effects of upper atmosphere space weather on the systems presented in this report.

COMMUNICATION SATELLITES

Satellites facilitate most means of civil and military communications. Cell phones, internet connections, television, and radio use communication satellites. By operating in a wide range of radio and microwave frequencies to relay messages to ground receiver stations or the end devices themselves, satellite communication (SATCOM) is also susceptible to UAP.
For example, satellite radio signals in the very HF (VHF, 30-300 MHz frequency range, 10-1 m spatial range) and above suffer degradation due to the background ionization. In turn, rapid fluctuations in the amplitude and phase of the radio signal can lead to repeated disruption of communications links with clear detrimental implications for businesses providing communications services and customers alike.

Ground-based Infrastructures

ASTRONOMICAL OBSERVATION SYSTEMS (LOFAR)

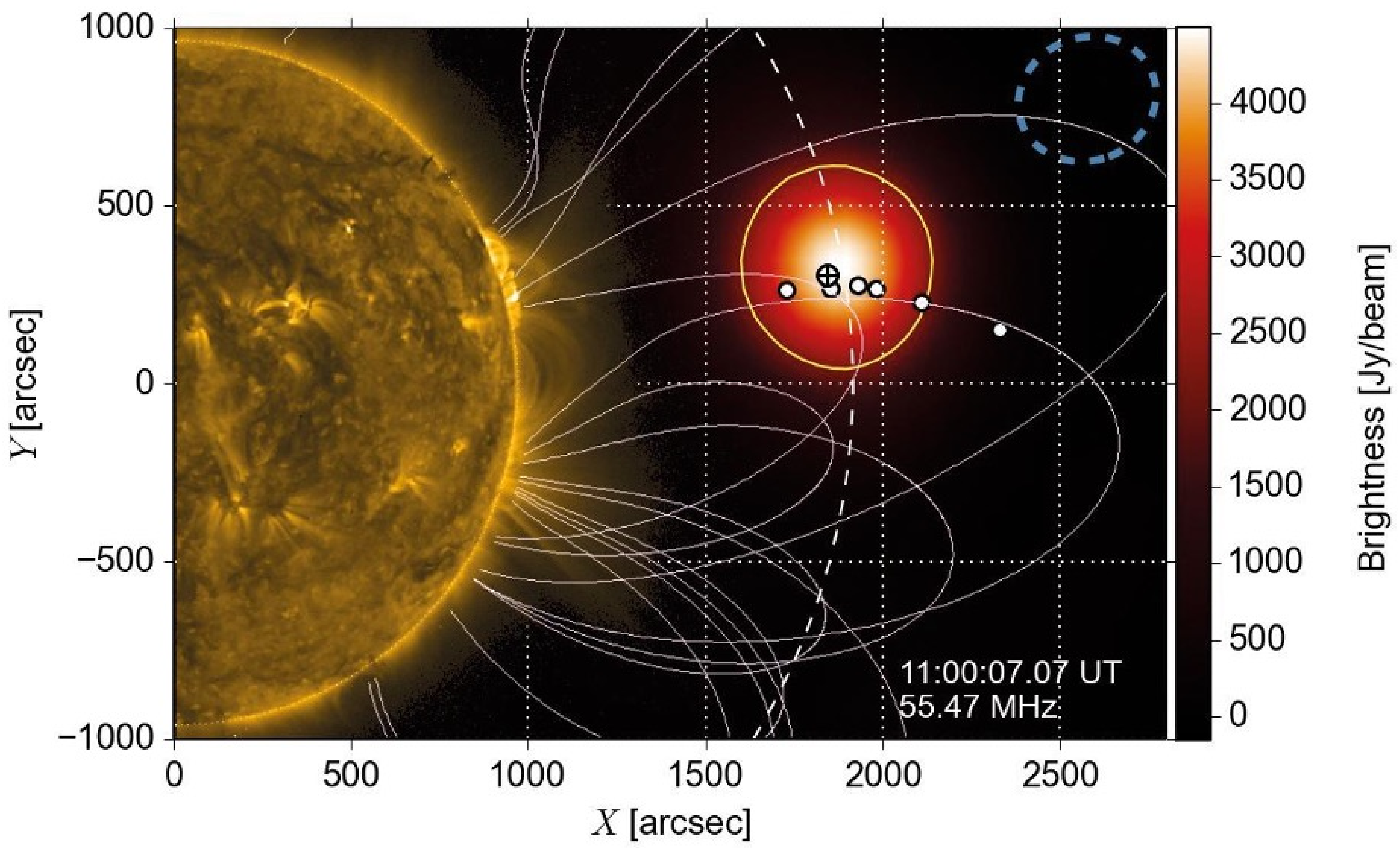

Figure 4. LOFAR's imaging spectroscopy of a solar type-III burst occurred in the frequency range of 30-60 MHz at 11:00 UTC on June 23, 2012.

LOFAR (Low-Frequency Array) is currently the largest radio telescope operating at the lowest frequencies detectable from Earth. Unlike single-dish telescopes, LOFAR is a multipurpose sensor network infrastructure that can handle huge data volumes allowing astronomers to engage in multiple lines of research at once.
Solar science and space weather are among them. The Sun's activity appears not only in the 11-year Sunspot cycle but also in short-duration eruptions such as flares and coronal mass ejections (CMEs). These events are accompanied by enhanced radio emissions from the Sun, especially in the frequency range (30-240 MHz) covered by LOFAR (Figure 4).

However, the view of the radio universe at the VHF frequencies of LOFAR is strongly affected by the Earth's ionosphere. Radio waves can get refracted and scattered in this region due to the intensification of auroral jets and ionospheric plasma bubbles. The effect for astronomers is that the images they are trying to take of distant radio sources can be heavily distorted. For comparison, think of looking at a pebble through troubled water.

PNT WITH GNSS AND GROUND-BASED AUGMENTATION SYSTEMS

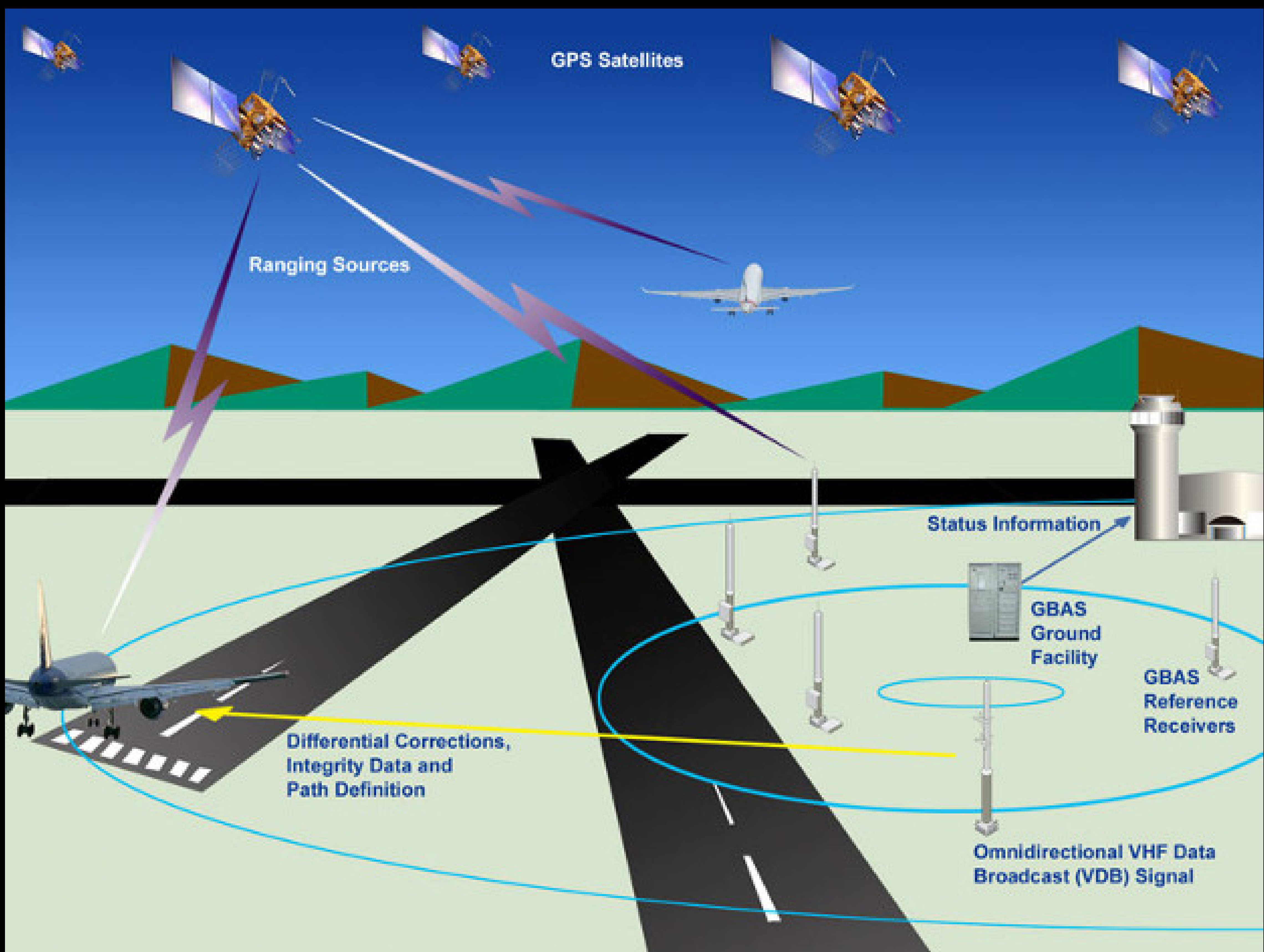

Figure 5. GBAS architecture (Source: Navipedia/FAA).

GNSS is an infrastructure that allows users with a compatible device worldwide to determine their position, velocity, and timing by processing signals from satellites. Global constellations include the Unit Global Positioning System (GPS), Russia's Global Navigation Satellite System (GLONASS), EU's Galileo, and China's BeiDou. GNSS provide PNT services fundamental to modern societies and their economies.

All GNSS communicate with ground-based receivers using radio transmitters. A signal transmitted by the satellite travels through the Earth's ionosphere and reaches the receiver. Under normal conditions, the GNSS receiver locks on to the signal and uses it to compute its location. However, turbulent ionospheric conditions, summarized in Table 1, can generate inaccuracy in the calculated position or time, cause temporary loss of lock in the receiver, or even induce complete outages.

The so-called augmentation systems are used to overcome ionospheric delays inducing ranging errors. The augmentation of a GNSS is a method for improving the GNSS' performances, such as integrity, continuity, accuracy, or availability, by computing and broadcasting differential corrections and integrity-related information to, e.g., an aircraft performing precision approach operations (Figure 5). Nonetheless, extreme ionospheric conditions would seriously degrade GBAS performance, too.

TERRESTRIAL RADIO SYSTEMS (HF COMMUNICATIONS)

All radio communication methods are based on electromagnetic wave propagation, which varies with the frequency of the radio waves and the medium used to carry them. The medium can be the troposphere, ionosphere, or outer space.

HF communication systems use the ionosphere as a natural high-altitude reflector to cover large distances without an intermediate ground-based or satellite infrastructure. During the daytime, the path loss through the ionosphere increases with decreasing frequency due to D-layer absorption, but too high-frequency waves will pass through the ionosphere. Therefore, civil and military radiofrequency system operators must select the right HF frequency depending on the ionospheric reflection properties (Cander, 2019).

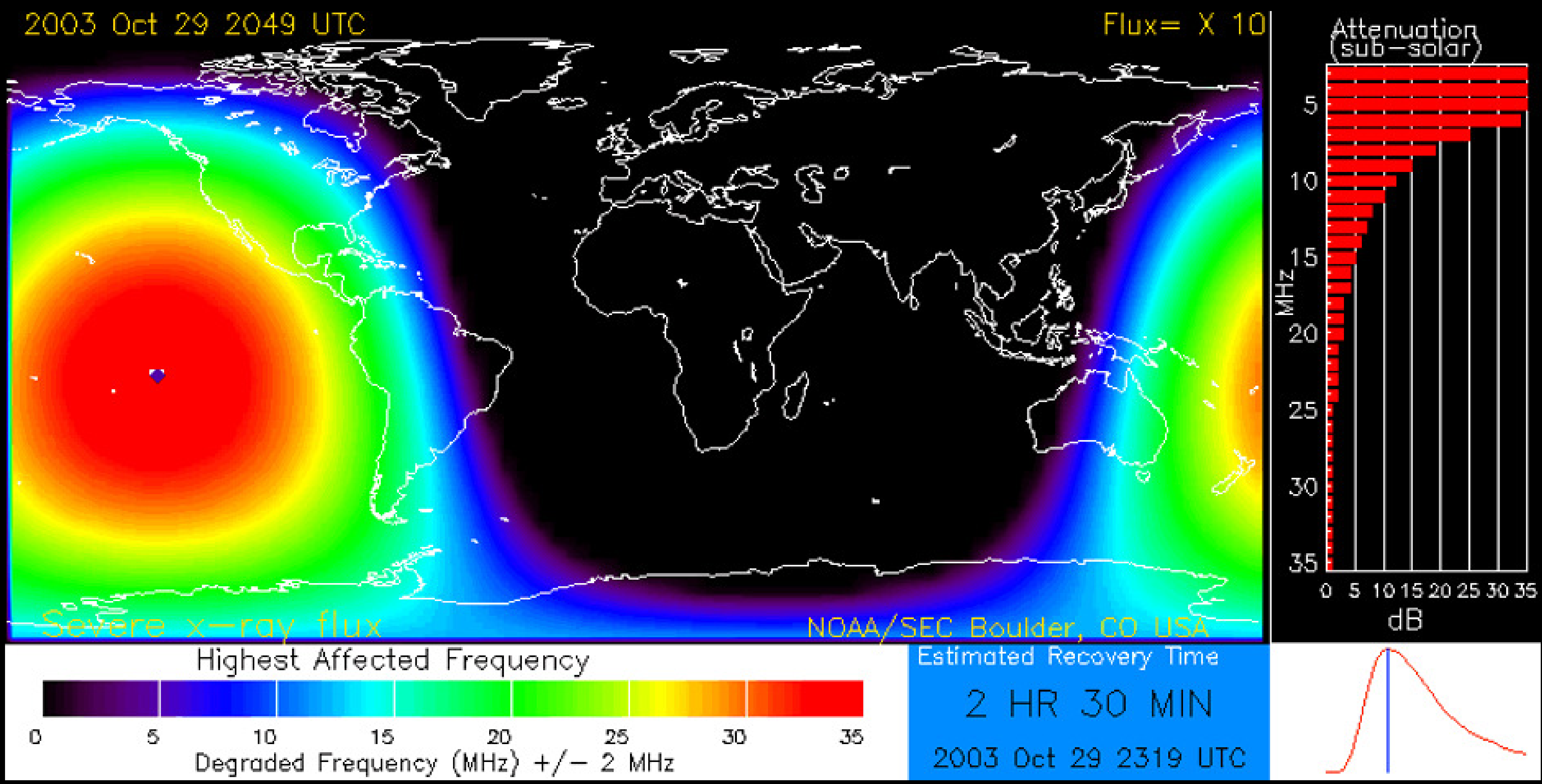

Figure 6. HF absorption during the intense October 29, 2003, solar storm. Due to geometric effects, the D-region ionization is most significant at the subsolar point, where the Sun is directly overhead. The amount of ionization and absorption falls with distance away from the subsolar point, reaching zero at the day/night terminator. The night-side of Earth is unaffected (ICAO, 2015).

FOCUS: Communications for Humanitarian operations and NGOs

In remote regions of Lower- and Middle-Income Countries (LMIC), where land-based telecommunication infrastructure is lacking altogether, HF radiocommunication provides a cheap alternative to satellite communications for which the equipment and usage fees are often unaffordable. Some Non-Governmental Organizations (NGOs), such as Médecins sans Frontières (MSF), use HF communications to provide primary healthcare in such countries. HF communications are also used as a quickly established communication infrastructure when the existing infrastructure is destroyed by a significant natural or man-made disaster (Comfort et al., 2006). To quickly cover a large area by ionospheric radio wave propagation, a wave frequency below the peak plasma frequency of the ionosphere must be used; a method referred to as Near Vertical Incidence Skywave (NVIS) propagation (Witvliet and Alsina-Pagès, 2017).
It may be clear that an, e.g., a Short Wave Fade-out will create a security hazard for an MSF ambulance that is on its way in a conflict zone or will stall relief work of rescue workers in a disaster area.

The ionosphere's electron density condition is critical in establishing a successful radio link. It depends on the diurnal cycle, the seasons, the geographical location, and the space weather conditions. During quiet space weather conditions, the vertical and geographical distribution of the electron density is highly predictable (Bilitza et al., 2017), allowing for precise frequency and range planning for the desired radio links. However, disturbed geomagnetic conditions, solar X-ray flares, and solar particle emissions (SPE) may vary the usual electron density distribution or cause heavy absorption, jeopardizing radio communications.

Many sectors, including defense, Search and Rescue services, broadcasters, marine transport, and aviation, depend on HF communications availability for their operations. For example, HF is the primary means of radio communications above approximately 82° latitude in aviation. Still, airlines also use it at low-mid latitudes during trans-oceanic flights and routes where line-of-sight VHF communication is not an option (ICAO, 2014). This is why the International Civil Aviation Organization (ICAO) relies on the PECASUS' Global Space Weather Center for aviation 24/7 operations for information on space weather that has the potential to affect, among other services, HF communications. Figure 6 shows the effect of a powerful solar flare that happened on October 29, 2003, resulting in lost or degraded HF communications over the continental US for several hours.


19L
19R
19R-1L
TAXI

5. Quantifying socioeconomic impacts: How far have we come?

The previous sections highlight how disturbances in the Earth's upper atmosphere can interfere with the continuous functioning of critical technological infrastructures in space and on the ground. Let us think of the ever-increasing number of active satellites orbiting the Earth (Figure 7), enabling broadband satellite communications, EO, and PNT, among other services. Or consider aviation's dependence on HF communications, the primary and, in some cases, sole means of communicating over the poles (ICAO, 2015).

However, to help inform cost-benefit assessments for resilience, decision-makers in government and industry need reliable information from economic analyses on the adverse impacts of the upper atmosphere phenomena. Nevertheless, despite the risks and our dependence on such technologies, efforts to quantify the socioeconomic implications of the UAP, or, more generally, of space weather events, have been, to date, relatively piecemeal in comparison to the existing literature on terrestrial natural hazards such as hurricanes, earthquakes, or tsunamis (Oughton, 2018, Eastwood et al., 2017) for which the economic impacts are comparable (Figure 8).

The reasons behind this unbalance are multiple and range from modern society's lack of experience with extreme space weather events (Table 3) to affected industries' uneasiness in sharing potentially business-sensitive data that researchers could use in simulations. Also, the difficulty in predicting the size and location of UAP impact zone is an issue (Oughton, 2018, Worman et al., 2018).

Nonetheless, in recent years, a few studies have advanced our understanding of the nature of impacts, posing the basis for defining socioeconomic impacts indicators (Worman et al., 2018) and quantitative methodologies (Eastwood et al., 2018, Oughton, 2019) to capture the economic impacts caused by UAP.

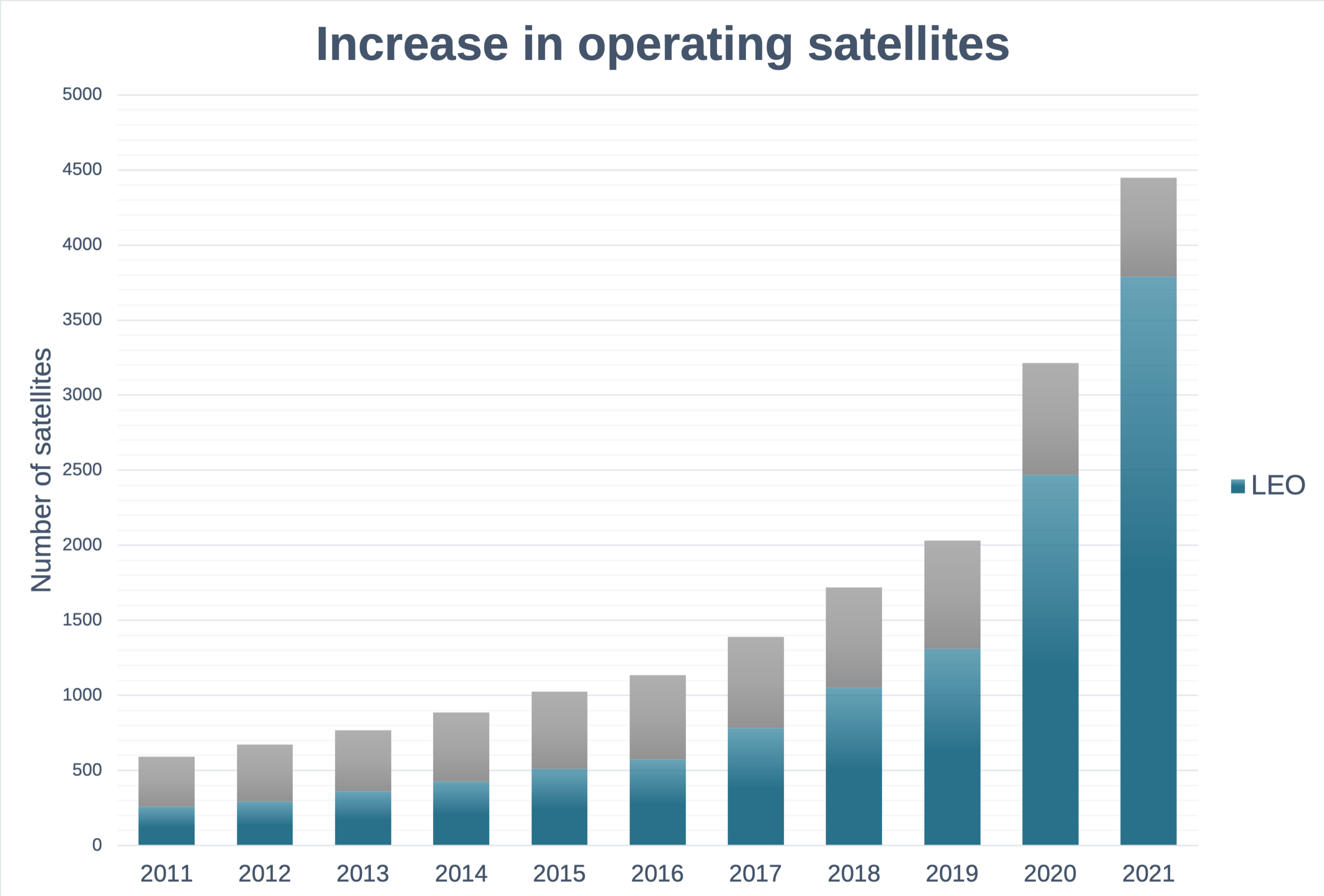

Figure 7. The number of satellites orbiting the Earth registered a 650% increase from 2011 to 2021, while the number of LEO satellites saw a 1350% growth over the same period. Data from "Union of Concerned Scientists Database," retrieved on 09/02/2022 from https://www.ucsusa.org/resources/satellite-database.

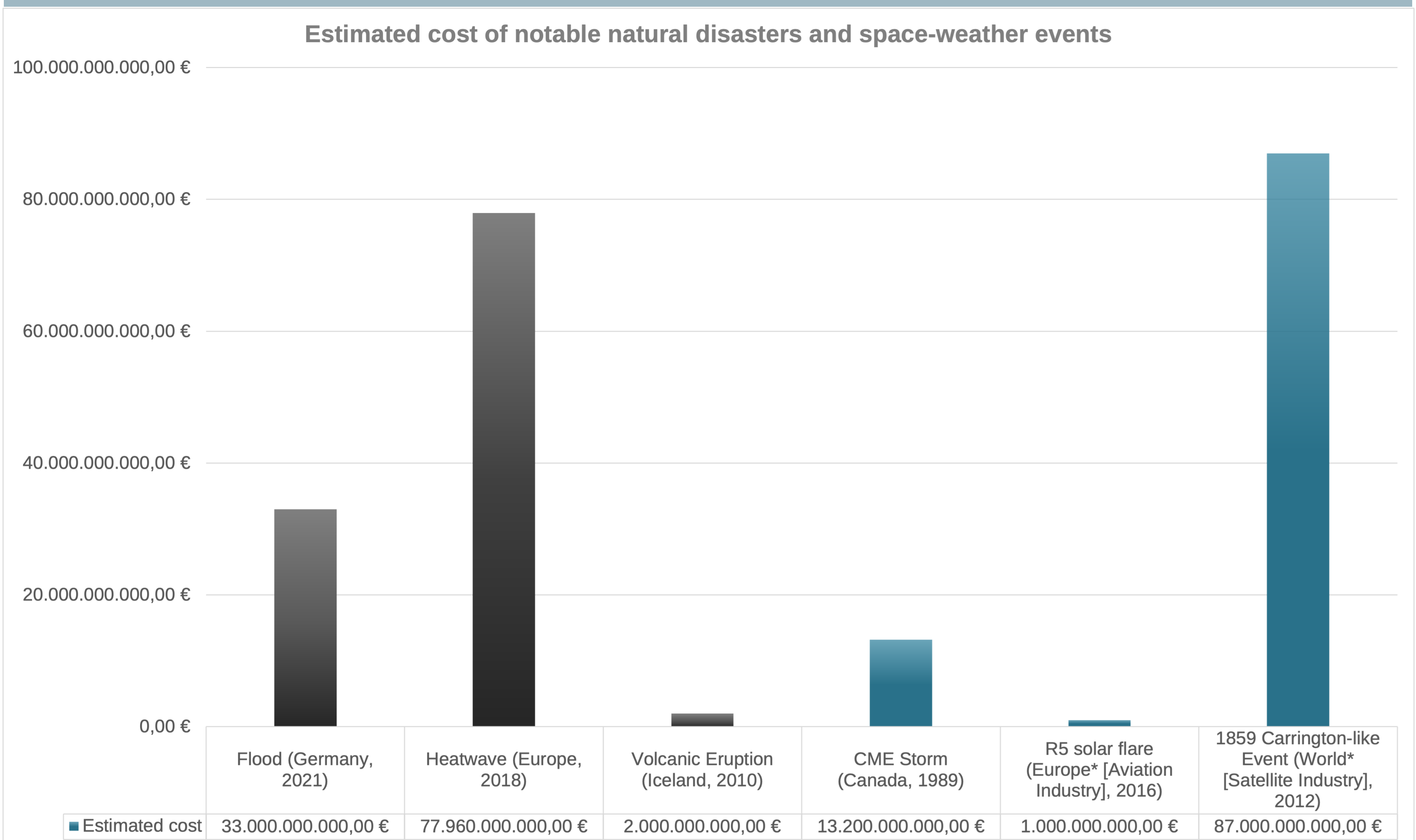

Figure 8. Space weather is a low probability high-impact event, with costs to society not dissimilar from those caused by major natural disasters.

Year	Impact	References
2006	December 2006 event had critical impacts on GNSS users on the sunlit side of the Earth, with disruption for tens of minutes up to an hour.	Cerruti et al., 2008; Carrano et al., 2009
2003	The Halloween Storms included a mix of CMEs and flares. This storm also led to a radio blackout of HF communications and disruption to GPS systems. Total loss of ADEOS/MIDORI 2 LEO satellite due to solar array.	Pulkkinen et al., 2005; Tsurutani et al., 2005; Bergeot et al., 2010
2000	The Bastille Day Event saw a massive CME and flare. The ISS' orbital perigee was reduced by 15km. Horizontal position errors of 20-40m were recorded for several differential GPS.	Tsurutani et al., 2005; Odenwald et al., 2006
1958	Transatlantic communications were disrupted between Newfoundland and Scotland. There was a blackout in the Toronto area.	Anderson, 1978; Lanzerotti and Gregori, 1986
1940	Damage was caused to the US telephone system and reported effects on the electricity network.	Harang, 1941; Davidson, 1940
1872	Auroras were sighted as low as 10-20° geomagnetic latitude, with significant recordings in Mumbai.	Moos, 1910a; 1910b; Uberoi, 2011
1870	A large storm produced aurora sightings in Lisbon and Coimbra (Portugal), Greenwich (UK), Munich (Germany), and Helsinki (Finland).	Vaquero et al., 2008
1859	The Carrington Event: there was significant disruption caused to telegraph systems across the globe, and auroras were witnessed down to very low latitudes.	Boteler, 2006; Siscoe et al. 2006; Green and Boardsen, 2006; Ribeiro et al. 2011; Rodger et al., 2008; Saiz et al., 2016; Silverman, 2006; Tsurutani et al., 2003

Table 3. Summary of historical storms provoking upper atmosphere disturbances inducing adverse effects on technologies (adapted from Oughton, 2018).

Indeed, the costs associated with UAP are of different types (direct, indirect, mitigation costs) and due to various economic actors (infrastructure operators, commercial and industrial customers, households), as shown in Figure 9 (Oughton, 2018).

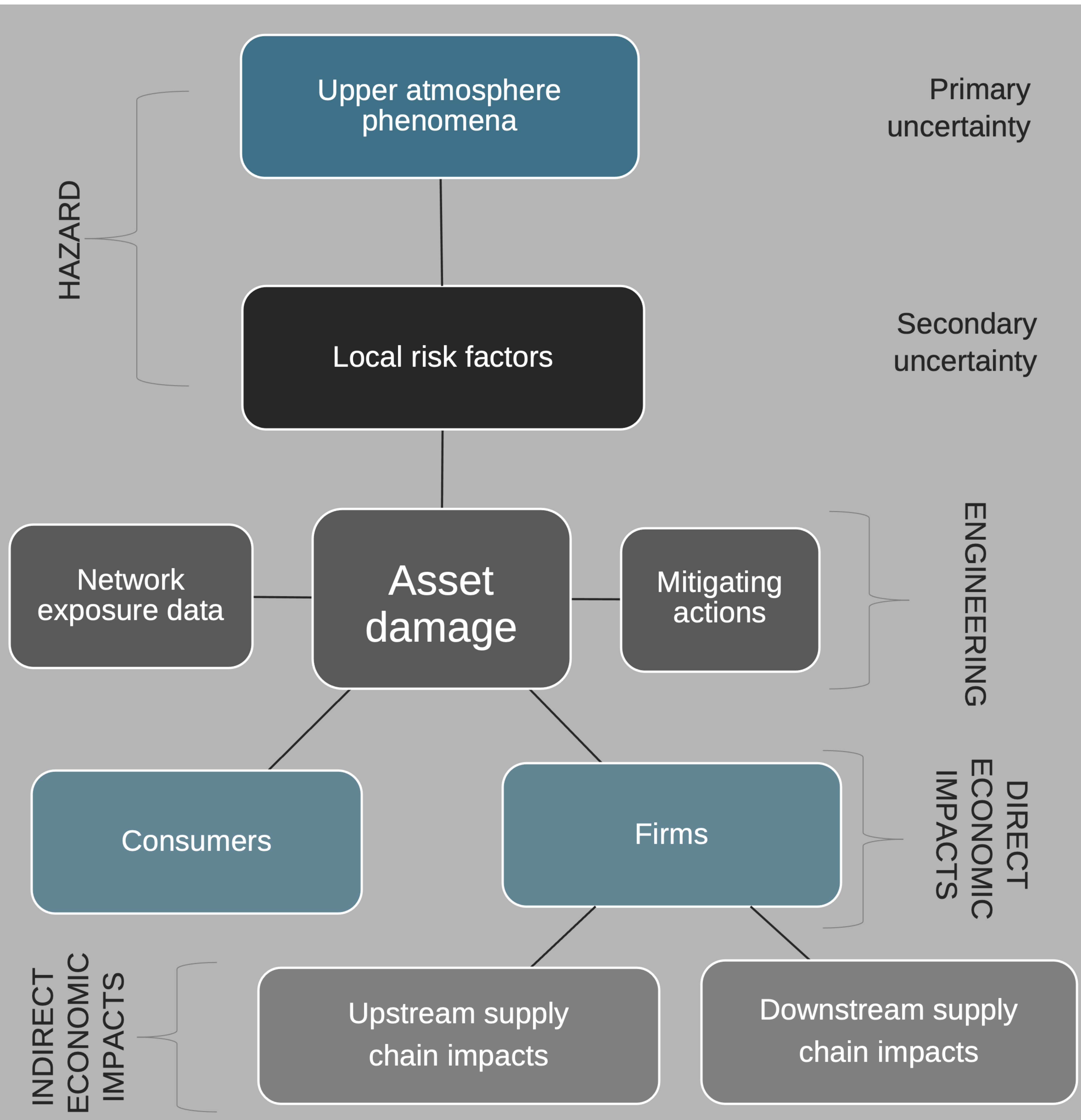

Figure 9. The economic costs associated with upper atmosphere phenomena (adapted from Oughton, 2018).

Here are the cost estimates based on a systematic review of the sectors relevant to this report.

LEO SATELLITES

Quantifying the impacts of UAP on the operation of satellites operating in LEO is not an easy task. It varies broadly according to the assumptions (e.g., one or more asset losses) and the severity of the space-weather event considered.

While LEO satellites are less vulnerable to cumulative dosage or anomalies caused by SPEs than those in GEO and MEO orbits, reducing costs associated with defensive investments, their most significant risk comes from atmospheric friction and orbit decay caused by variable drag forces in the thermosphere (atmospheric drag). For example, Odenwald et al. (2006) assessed that the increased atmospheric drag caused by a superstorm akin to the 1859-Carrington event would cause the premature de-orbit of approximately 97 LEO satellites, worth an estimated $16 billion (2005 value). Likewise, ABT Associated (2017) found that an event of similar magnitude, causing the loss of 10 to 100 satellites globally, would have a staggering global direct economic impact of $4-$200 billion by combining the lost satellite assets' value and their lost service revenues.

Since then, with the advent of commercial "mega-constellations," the LEO domain has become only more crowded: Eighty-five percent of all active satellites move in LEO orbit, rendering the effect of a severe storm even more dramatic due to the exponentially increasing risk of cascading collisions (Kessler et al., 2010, Berger et al., 2020).

Moreover, even mild events can negatively affect business operations, like the incident on February 3rd, 2022, highlights, when forty Starlink satellites were lost to thermospheric drag during the insertion phase.

Another risk associated with mega-constellations, the majority of which will form new telecommunications systems, is that multiple spacecraft launched within a relatively short time will feature the same or similar components. Therefore, if previously unidentified issues emerge, they could cause a loss of capability for multiple space missions or even lead to the failure of satellites (LE, 2019).

Moreover, the increasing use of Commercial-Off-The-Shelf (COTS) components – whose wider availability reduces manufacturing lead times - raises doubts about the durability of materials to withstand high-velocity impacts and harsh space weather, as exemplified by the failure of the SumbandilaSat satellite in 2012 . Therefore, a quantitative assessment of the downstream implications of the vulnerability of mega-constellations design is needed.

€3 BLN: THE AMOUNT OF REVENUES GENERATED BY EO DATA AND SERVICES

FOCUS: Earth Observation Satellites

Almost all satellites for EO purposes lie in LEO (UCS, 2022). With an estimated asset value of $30 million per satellite (ABT Associates, 2017) and global demand for EO data and value-added services generating almost €3 billion in revenues (EUSPA, 2022), the consequences of losing even one EO satellite would be costly.

PNT WITH GNSS AND GROUND-BASED AUGMENTATION SYSTEMS

In 2021, the global demand for GNSS equipment generated €200 billion between devices and services revenues, with Europe holding a 20% market share (EUSPA, 2022).

However, GNSS and GBAS are susceptible to UAP that, in a worst-case scenario, could render PNT services unavailable to users, commercial and not, for up to several days (Table 2).

	Estimated costs to application by geographical area (Reference)		
GNSS Application	Europe (Pwc, 2016)	USA (ABT Associates, 2017)	Canada (HAL, 2019)
Precision Agriculture	Not stated	$30-100 million	$0.5 million
Surveying	€197,5 million	$30-100 million	$0.8-1.7 million
Road Transport and Logistics	€0.8-2.4 billion	$20-100 million	Not stated

Table 4. The cost associated with 1-3 days to 14 days GNSS outage in three main commercial sectors using GNSS equipment.

Table 4 reports the estimated cost associated with a one to 14-day GNSS outage in three main commercial sectors over which GNSS PNT has a dominant influence. The figures for the precision agriculture and surveying sectors represent either the direct costs of suspending or delaying operations (PwC, 2016, HAL, 2019) or the benefits of using GNSS equipment (ABT Associates, 2017). By contrast, PwC (2016) reports the impact on European GDP from 3 days of GPS loss leading to 14% of the sector not operating in full efficiency (cost calculated with input-output analysis). One can note how the estimates vary across sectors and geographical areas, depending on the suite of mitigating actions in place; the road and logistics sector would be the worst hit.

TERRESTRIAL RADIO SYSTEMS

In the reviewed literature, cost estimates for terrestrial radio systems typically focus on the impacts on aviation of HF radio waves absorption in the upper atmosphere. At the same time, HF communications blackout due to turbulent ionospheric conditions can affect, among others, disaster-risk management operations (e.g., September 2017's hurricane response in the Caribbean (Redmon et al., 2018)). Still, there is no cost-based evidence in this area.

AVIATION

In aviation, HF communications remain the primary and, in some cases, sole means of communicating over the poles (ICAO, 2015), and, despite the use of line-of-sight datalink systems and Satcom transmission, the safest and quickest options in many emergencies (Hapgood et al., 2020). Table 5 presents the findings concerning the costs of delaying, canceling or rerouting flights for a total blackout of HF radio frequencies in Europe, the USA, and Canada.

	Aviation (Reference)		
Costs	Europe (Pwc, 2016)	USA (ABT Associates, 2017)	Canada (HAL, 2019)
Cost of delaying, canceling, or rerouting flights	€812 million	$1-30 million	Not stated
Passengers' value of lost time	€14,7 million	$6-200 million	Not stated
Total	€0.83 billion	$7-230 million	$1.75 billion

Table 5. Aviation economic impacts. Impacts for Canada are computed as the decrease of national GDP by 0.092%, resulting from a combination of increases in airline costs and reductions in labor productivity.

Depending on the intensity and type of UAP, the areas affected and the time extension of the outage could vary: the blackout could last for two or three hours in all low- and mid-latitude regions on the dayside of the Earth or several days at high-latitudes (Hapgood et al., 2020). As a consequence of even more severe UAP, there would be an economic impact on all aviation in the considered regions, not just in the polar sector.

In summary, despite the risks posed by UAP to critical space- and ground-based technologies, the science of quantifying their socioeconomic impacts is not yet mature, partly for the lack of important modeling information. Nevertheless, a few notable studies have certainly advanced our understanding of this under-researched hazard, nonetheless focusing only on a subset of infrastructures and phenomena affecting them, often proposing estimates of direct costs to commercial users (Figure 10) without fully exploring the total costs associated with UAP.

Entity	**Cost Type**	**Type of estimated cost per infrastructure**			
		Space-borne infrastructure	**Ground-based infrastructure**		
		LEO Satellites	PNT	AOS	TRS
Infrastructure network operator	Direct	✓	✓		
	Indirect				
	Mitigation	✓			
Commercial and industrial customers	Direct	✓	✓		✓
	Indirect		✓		✓
	Mitigation				
Households	Direct				✓
	Indirect				
	Mitigation				

Figure 10. Type of estimated costs analyzed in the literature, per infrastructure.

6. Glossary

Term	Definition
Auroral electrojet	A current that flows in the ionosphere in the auroral zone
Carrington event	It was the most significant solar storm on record. It took place from 1-3 September 1859 and is named after British astronomer Richard Carrington
Coronal mass ejection	A large burst of solar wind plasma ejected into space
Doppler shift	A change in the perceived frequency of a radiated signal caused by the motion of the source relative to the observer
Extreme ultraviolet	A portion of the electromagnetic spectrum from approximately 10 to 100 nm
Faraday rotation	A phenomenon whereby the polarization plane of radio waves rotates due to magnetic flux lines and electrons in the ionosphere, resulting in different phase velocities for left- and right-hand circularly polarized waves. The rotation angle is roughly in inverse proportion to the square of the frequency. This rotation does not affect the received powers of circularly polarized waves but reduces received powers for linearly polarized waves. Faraday rotation can degrade the quality of low-frequency space-borne SAR data, making estimation and correction of this effect a prerequisite for data quality continuity.
Geomagnetic storm	A worldwide disturbance of the Earth's magnetic field induced by a solar storm
Geostationary orbit	A circular orbit 35,900 km above the Earth's surface where most telecommunications satellites are located. Satellites in GEO orbit appear stationary relative to the rotating Earth
Interplanetary magnetic field	The solar magnetic field carried by the solar wind to the planets and beyond
L1 Lagrangian point	The point where the gravitational forces of the Sun and Earth balance

Plasma bubbles	Irregular and extremely low electron density regions in the equatorial and low-latitude ionosphere caused by the Rayleigh–Taylor instability. Plasma bubbles affect radio wave propagation from satellites to the ground and differential GNSS correction. In addition, plasma irregularities inside plasma bubbles lead to signal scintillation.
Polar cap absorption	An anomalous condition of the polar ionosphere where HF and VHF (3-300 MHz) radio waves are absorbed and LF and VLF (3-300 kHz) radio waves are reflected at lower altitudes than usual. PCAs generally originate with major solar flares, beginning within a few hours of the event and maximizing within a day or two of onset. As measured by a riometer, the PCA event threshold is 2 dB of absorption at 30MIlz for daytime and 0.5 dB at night. In practice, the absorption is inferred from the proton flux at energies greater than 10 MeV so that PCAs and proton events are simultaneous. However, the transpolar radio paths may be disturbed for days, up to weeks, following the end of a proton event
Ring current enhancement	In the magnetosphere, a region of current that flows from east to west in a disk-shaped region near the geomagnetic equator in the outer of the Van Allen radiation belts. The current is produced by the gradient and curvature drift of the trapped charged particles. The ring current is greatly augmented during magnetic storms because of the hot plasma injected from the magnetotail. This increase in the ring current causes a worldwide depression of the horizontal component of the geomagnetic field during a magnetic storm
Riometer	A specially designed ground-level radio receiver for continuous monitoring of cosmic noise. The cosmic noise absorption in the polar regions is very sensitive to the solar low-energy cosmic ray flux. Absorption events are known as PCAs (polar cap absorption) and are primarily associated with major solar flares

Scintillation	Describes a degraded condition of radio propagation characterized by a rapid variation in amplitude and phase of a radio signal (usually on a satellite communication link) caused by abrupt variations in electron density anywhere along the signal path. It is positively correlated with spread F and, to a lesser degree, sporadic E. Scintillation effects are the most severe at low latitudes but can also be a problem at high latitudes, especially in the auroral oval and over the polar caps
Short Wave Fade-outs (SWF)	Earth-directed solar X-ray flares will cause more widespread absorption of medium wave and lower HF (1-20 MHz) radio waves at lower and mid-latitudes on the side of the Earth that is directed towards the Sun. The intense X-ray radiation suddenly increases the ionization in the D-region of the ionosphere and interacts with radio waves entering it, absorbing their energy through collisions with other ions and neutral atoms. This phenomenon, also known as a Sudden Ionospheric Disturbance or the Mögel-Dellinger effect (Traxler et al., 2014), suddenly increases the absorption of radio waves. The absorption is often so high (often exceeding 60 dB) that even the strongest radio signals are fully absorbed (Witvliet et al., 2016). As a result, the SWF entirely cuts off each HF radio circuit on the sunlit side of the earth. The onset of an SWF is very rapid, mostly minutes, while its duration depends on the intensity and duration of the solar X-ray burst and will range from half an hour to several hours.
Solar energetic particles	High-energy particles coming from the Sun
Solar flare	A brief, powerful eruption of particles and intense electromagnetic radiation from the Sun’s surface
Solar wind	The constant stream of charged particles, mainly protons and electrons, emitted by the Sun at high velocities, its density and speed varying during periods of solar activity

Sporadic E-layer	Transient, localized patches of relatively high electron density in the E region of the ionosphere significantly affecting radio-wave propagation. Sporadic E can occur during daytime or nighttime and varies markedly with latitude. Es can be associated with thunderstorms, meteor showers, solar, and geomagnetic activity.
Spread F	A condition of the F region of the ionosphere caused by patches of ionization that scatter or duct radio signals, characterized on ionograms by a wide range of heights of reflected pulses. In equatorial latitudes, spread F is most commonly observed at night and might negatively correlate with geomagnetic activity. Spread F occurs throughout the daytime at high latitudes and is positively correlated with magnetic activity. The latitude of minimum occurrence of spread F is near 30 degrees magnetic latitude.
Sudden ionospheric disturbances	Any of several radio propagation anomalies due to ionospheric changes resulting from solar or geophysical events. Anomalies include short wave fades, enhancements of atmospherics, phase shifts, cosmic noise absorptions, and signal enhancements.
TEC gradients	Spatial plasma density gradients can be represented by the Total Electron Content, TEC, changes across latitude or longitude (TECU/deg), or their changes over distance (TECU/km). The inhomogeneity of ionospheric electron distribution can cause, e.g., GNSS signals scintillation and additional travel time delays. Radicella et al. (2004) and Nava et al. (2007) showed how horizontal gradients of vertical TEC contribute to positioning error, with TEC gradients as low as 0.01 TECU/km already reducing the accuracy of an L-band cross-track interferometer by 1-2 m. Higher-order perturbations of the electron plasma lead to additional errors that vary nonlinearly with the length of the interferometric baseline.

Traveling ionospheric disturbances	Perturbations of the ionospheric electron density driven by acoustic gravity waves (AGW). They originate from various sources such as solar events (geomagnetic storms, solar flares) or terrestrial events (hurricanes, tornados, volcanos, Earthquakes, rocket launchers, etc.). Based on their phase velocity and wave period, AGWs and classical TIDs are often classified into medium- and large-scale waves (MSTID/LSTID). LSTID and MSTID both impact HF radio systems and are generally considered the largest source of uncertainty in predicting the behavior of HF systems. Given the multiple sources of gravity waves in both the troposphere and thermosphere and the variability of the medium through which they propagate, it is challenging to predict TIDS occurrences even on a statistical basis.

7. List of abbreviations and acronyms

Acronym	Meaning
AE	Auroral electrojet index of auroral zone magnetic activity
AGW	Acoustic gravity wave
CH	Coronal Hole
CME	Coronal Mass Ejection
COTS	Commercial-Off-The-Shelf
EGNOS	European Geostationary Navigation Overlay Service
EO	Earth Observation
ESA	European Space Agency
EUSPA	European Union Agency for Space Programme
FAA	Federal Aviation Administration
GBAS	Ground-based augmentation systems
GEO	Geostationary orbit
GLONASS	GLObal NAvigation Satellite System - GLObalnaya NAvigatsionnaya Sputnikovaya Sistema) A satellite-based radio navigation system
GMD	Geomagnetic disturbance
GNSS	Global Navigation Satellite Systems
GPS	Global Positioning System
HF	High-frequency (3-30 MHz, 100-10m)
HSS	High-speed stream
ICAO	International Civil Aviation Organization
ICME	Interplanetary Coronal Mass Ejection
IMF	Interplanetary magnetic field
Kp	Planetary K-index for geomagnetic storms
L1	First lagrangian point
LEO	Low Earth orbit

LF	Low frequency (30-300 kHz, 10-1km)
LOFAR	Low-frequency array
MEO	Medium Earth orbit
MF	Medium frequency (300 kHz to 3 MHz, 1km to 100m)
MHz	A Megahertz
NOAA	National Oceanic and Atmospheric Administration
PCA	Polar cap absorption
PNT	Positioning, navigation, and timing
ROTI	Rate of Ionospheric Total Electron Content index
SAR	Synthetic Aperture Radar
SATCOM	Satellite communications
SBAS	Satellite-based augmentation systems
SEE	Single event effects
SEP	Solar energetic particles
SEU	Single event upset
SIDS	Sudden ionospheric disturbances
SPE	Solar particle events
SRB	Solar flare solar radio burst
SW	Short wave
TEC	Total Electron Content
TECU	Total Electron Content units
TIDS	Traveling ionospheric disturbances
UAP	Upper atmosphere phenomena
UHF	Ultra-high frequency (300 MHz to 3 GHz, 1m to 10 cm)
UTC	Universal coordinated time
VHF (VLF)	Very high (low) frequency (30-300 MHz, 10-1m; 3-30 kHz, 100-10km)
WAAS	US wide-area augmentation system

8. References

Socioeconomic impacts in "Figure 8"

Flood, Germany, 2021:
https://www.munichre.com/en/company/media-relations/media-information-and-corporate-news/media-information/2022/natural-disaster-losses-2021.html

Heatwave, Europe, 2018:
García-León, D. et al., (2021), “Current and projected regional economic impacts of heatwaves in Europe,” Nature Communications, https://doi.org/10.1038/s41467-021-26050-z

Volcanic Eruption, Iceland, 2010:
Ulfarsson, G.F, and Unger, E.A., (2011), “Impacts and Responses of Icelandic Aviation to the 2010 Eyjafjyallajökull Volcanic Eruption: a Case Study”, Transportation Research Record Journal of the Transportation Research Board, 2214, 144-151, doi: 10.3141/2214-18

CME, Quebéc, 1989:
Worman, S., Taylor, S., Onsager, T., Adkins, J., Baker, D. N., & Forbes, K. F. (2018). The social and economic impacts of moderate and severe space weather. Extreme Events in Geospace: Origins, Predictability, and Consequences. Elsevier Inc. https://doi.org/10.1016/B978-0-12-812700-1.00029-7

1859-Carrington like event, World (Satellite Industry):
Odenwald, S., Green, J., & Taylor, W. (2006). Forecasting the impact of an 1859-caliber superstorm on satellite resources. Advances in Space Research, 38(2), 280–297. https://doi.org/10.1016/j.asr.2005.10.046

R5 flare, Europe (Aviation industry):
PwC. (2016). Summary of CBA Results by domain Summary Charts Sensitivity analyses Downstream market.

Socioeconomic impacts

Abt Associates. (2017). Social and Economic Impacts of Space Weather in the United States. Retrieved from https://www.weather.gov/media/news/SpaceWeatherEconomicImpactsReportOct-2017.pdf

Eastwood, J. P., Biffis, E., Hapgood, M. A., Green, L., Bisi, M. M., Bentley, R. D., et al. (2017). The Economic Impact of Space Weather: Where Do We Stand? Risk Analysis, 37(2), 206–218. https://doi.org/10.1111/risa.12765

Eastwood, J. P., Hapgood, M. A., Biffis, E., Benedetti, D., Bisi, M. M., Green, L., et al. (2018). Quantifying the Economic Value of Space Weather Forecasting for Power Grids: An Exploratory Study. Space Weather, 16(12), 2052–2067. https://doi.org/10.1029/2018SW002003

HAL. (2019). Space Weather Socioeconomic Impact Study on Canadian Infrastructure - Final Report.

Hapgood, M., Angling, M., Attrill, G., Burnett, C., Cannon, P., Gibbs, M., et al. (2020). Summary of space weather worst-case environments, 56. Retrieved from http://purl.org/net/epubs/work/25015281vv

London Economics. (2019). NewSpace: Bringing the frontier closer to home.

MacAlester, M. H., & Murtagh, W. (2014). Extreme Space Weather Impact: An Emergency Management Perspective. Space Weather, (12), 530–537. https://doi.org/10.1002/ 2014SW001095.

Odenwald, S., Green, J., & Taylor, W. (2006). Forecasting the impact of an 1859-calibre superstorm on satellite resources. Advances in Space Research, 38(2), 280–297. https://doi.org/10.1016/j.asr.2005.10.046

Oughton, E. J. (2018). The Economic Impact of Critical National Infrastructure Failure Due to Space Weather. Oxford Research Encyclopedia of Natural Hazard Science, 1–36. https://doi.org/10.1093/acrefore/9780199389407.013.315

Oughton, E. J., Hapgood, M., Richardson, G. S., Beggan, C. D., Thomson, A. W. P., Gibbs, M., et al. (2019). A Risk Assessment Framework for the Socioeconomic Impacts of Electricity Transmission Infrastructure Failure Due to Space Weather: An Application to the United Kingdom. Risk Analysis, 39(5), 1022–1043. https://doi.org/10.1111/risa.13229

PwC. (2016). Summary of CBA: Results by domain Summary, Charts Sensitivity analyses, and Downstream market.

Worman, S., Taylor, S., Onsager, T., Adkins, J., Baker, D. N., & Forbes, K. F. (2018). The social and economic impacts of moderate and severe space weather. Extreme Events in Geospace: Origins, Predictability, and Consequences. Elsevier Inc. https://doi.org/10.1016/B978-0-12-812700-1.00029-7

Others

Alfonsi, L., Povero, G., Spogli, L., Cesaroni, C., Forte, B., Mitchell, C. N., et al. (2018). Analysis of the Regional Ionosphere at Low Latitudes in Support of the Biomass ESA Mission. IEEE TRANSACTIONS ON GEOSCIENCE AND REMOTE SENSING.

Anderson, C. W. (1978). “Magnetic Storms and Cable Communications.” Solar System Plasma Physics.

Bergeot, N., C. Bruyninx, P. Defraigne, S. Pireaux, J. Legrand, E. Pottiaux, and Q. Baire. (2010). “Impact of the Halloween 2003 Ionospheric Storm on Kinematic GPS Positioning in Europe.” GPS Solutions 15 (2): 171–80. https://doi.org/10.1007/s10291-010-0181-9.

Berger, T. E., Holzinger, M. J., Sutton, E. K., & Thayer, J. P. (2020). Flying Through Uncertainty. Space Weather, 18(1), 1–5. https://doi.org/10.1029/2019SW002373

Bilitza, D. et al.(2017). "International Reference Ionosphere 2016: From ionospheric climate to real‐time weather predictions." Space weather 15.2 : 418-429.

Boteler, D. H. (2006). “The Super Storms of August/September 1859 and Their Effects on the Telegraph System.” Advances in Space Research, The Great Historical Geomagnetic Storm of 1859: A Modern Look, 38 (2): 159–72. https://doi.org/10.1016/j.asr.2006.01.013.

Cander, L. R. (2019). Ionosphere Space Weather and Radio Propagation. In: Ionospheric Space Weather. Springer Geophysics. Springer, Cham. https://doi.org/10.1007/978-3-319-99331-7_8

Cannon, P. (2013). Extreme space weather: impacts on engineered systems and infrastructures. Royal Academy of Engineering. Retrieved from http://www.raeng.org.uk/news/publications/list/reports/Space_Weather_Full_Report_Final.PDF

Carrano, C. S., C. T. Bridgwood, and K. M. Groves (2009), Impacts of the December 2006 solar radio bursts on the performance of GPS, radio Sci., 44, RS0A25, doi: 10.1029/2008rs004071

Cerruti, A. P., P. M. K. Jr., D. E. Gary, A. J. Mannucci, R. F. Meyer, P. Doherty, and A. J. Coster (2008), Effect of intense December 2006 solar radio bursts on GPS receivers, Space weather, 6, S10D07, doi: 10.1029/2007SW000375.

Comfort, L. K., and Haase, T.W. (2006). "Communication, coherence, and collective action: The impact of Hurricane Katrina on communications infrastructure." Public Works Management & Policy 10.4: 328-343.

Davidson, W. F. (1940). “The Magnetic Storm of March 24, 1940 – Effects in the Power System.” Edison Electric Institute Bulletin 8: 365–366.

Green, James L., and Scott Boardsen. (2006). “Duration and Extent of the Great Auroral Storm of 1859.” Advances in Space Research, The Great Historical Geomagnetic Storm of 1859: A Modern Look, 38 (2): 130–35. https://doi.org/10.1016/j.asr.2005.08.054.

Harang, Leiv. (1941). “Maximalwerte Der Erdstromspannungen in Der Nähe Der Nordlichtzone Während Sehr Intensiver Erdmagnetischer Störungen (Maximum Values of Earth Current near the Auroral Zone during Very Intensive Geomagnetic Disturbances),(Written in German, with an English Summary).” Gerl. Beitr. Geophys 57: 310.

ICAO. (2015). Space Weather Effects in regard to International Air Navigation.

Kessler, D.J., Johnson, N.L., Liou, J.-C., Matney, M., (2010). The Kessler syndrome: implications to future space operations. In: 33rd Annual AAS Guidance and Control Conference, 6–10 February. American Astronautical Society, Breckenridge, Colorado.

Lanzerotti, L. J., and G. P Gregori. (1986). “Telluric Currents: The Natural Environment and Interactions with Man-Made Systems.” The Earth’s Electrical Environment, 232–257.

Moos, N. A. F. (1910a). Magnetic Observations Made at the Government Observatory Bombay 1847 to 1905 and Their Discussions, Part II, the Phenomenon and Its Discussion. Bombay, India: Gov. Cent. Press.

———. (1910b). Magnetic Observations Made at the Government Observatory, Bombay, for the Period 1846 to 1905 and Their Discussion, Part I, Magnetic Data and Instruments. Bombay, India: Gov. Cent. Press.

Nava, B., Radicella, S., Leitinger, R., and Coïsson, P. (2007). Use of total electron content data to analyze ionosphere electron density gradients, Advances in Space Research, 39, 1292–1297.

Pulkkinen, A., S. Lindahl, A. Viljanen, and R. Pirjola. (2005). “Geomagnetic Storm of 29–31 October 2003: Geomagnetically Induced Currents and Their Relation to Problems in the Swedish High- Voltage Power Transmission System.” Space Weather 3 (8): S08C03. https://doi.org/10.1029/2004SW000123.

Radicella, S. M., Nava, B., Coïsson, P., Kersley, L., and Bailey, G. J. (2004). Effects of gradients of the electron density on Earth-space communications, Annals of Geophysics, 47.

Redmon, R.J., Denig, W.F., Loto'aniu, P.T.M., Fuller-Rowell, D. (2018). Recent Geoeffective Space Weather Events and Technological System Impacts in Extreme Events in Geospace, Elsevier Inc, 587-609, ISBN 9780128127001, https://doi.org/10.1016/B978-0-12-812700-1.00024-8.

Ribeiro, P., J. M. Vaquero, and R. M. Trigo. (2011). “Geomagnetic Records of Carrington’s Storm from Guatemala.” Journal of Atmospheric and Solar-Terrestrial Physics, Space Climate, 73 (2–3): 308– 15. https://doi.org/10.1016/j.jastp.2009.12.017.

Rodger, Craig J., Pekka T. Verronen, Mark A. Clilverd, Annika Seppälä, and Esa Turunen. (2008). “Atmospheric Impact of the Carrington Event Solar Protons.” Journal of Geophysical Research: Atmospheres 113 (D23): D23302. https://doi.org/10.1029/2008JD010702.

Saiz, Elena, Antonio Guerrero, Consuelo Cid, Judith Palacios, and Yolanda Cerrato. (2016). “Searching for Carrington-like Events and Their Signatures and Triggers.” Journal of Space Weather and Space Climate 6: A6. https://doi.org/10.1051/swsc/2016001.

Silverman, S. M. (2006). “Comparison of the Aurora of September 1/2, 1859 with Other Great Auroras.” Advances in Space Research, The Great Historical Geomagnetic Storm of 1859: A Modern Look, 38 (2): 136–44. https://doi.org/10.1016/j.asr.2005.03.157.

Siscoe, G., N. U. Crooker, and C. R. Clauer. (2006). “Dst of the Carrington Storm of 1859.” Advances in Space Research, The Great Historical Geomagnetic Storm of 1859: A Modern Look, 38 (2): 173– 79. https://doi.org/10.1016/j.asr.2005.02.102.

Traxler, F. and Schlege, K. (2014). "Hans Mögel, transradio, and the Mögel dellinger effect." URSI Radio Science Bulletin 2014.351 : 53-57.

Tsurutani, B. T., W. D. Gonzalez, G. S. Lakhina, and S. Alex. (2003). “The Extreme Magnetic Storm of 1– 2 September 1859.” Journal of Geophysical Research: Space Physics 108 (A7): 1268. https://doi.org/10.1029/2002JA009504.

Tsurutani, B. T., D. L. Judge, F. L. Guarnieri, P. Gangopadhyay, A. R. Jones, J. Nuttall, G. A. Zambon, et al. (2005). “The October 28, 2003, Extreme EUV Solar Flare and Resultant Extreme Ionospheric Effects: Comparison to Other Halloween Events and the Bastille Day Event.” Geophysical Research Letters 32 (3): L03S09. https://doi.org/10.1029/2004GL021475.

Uberoi, Chanchal. (2011). “Geomagnetic Storms Over India: A Close Look at Historic Space Weather at Mumbai.” Space Weather 9 (8): S08005. https://doi.org/10.1029/2011SW000686.

Vaquero, J. M., M. A. Valente, R. M. Trigo, P. Ribeiro, and M. C. Gallego. (2008). “The 1870 Space Weather Event: Geomagnetic and Auroral Records.” Journal of Geophysical Research: Space Physics 113 (A8): A08230. https://doi.org/10.1029/2007JA012943.

Witvliet, B. A., and Alsina-Pagès, R.M. (2017). "Radio communication via Near Vertical Incidence Skywave propagation: an overview." Telecommunication systems 66.2: 295-309.

Witvliet, B. A., et al. (2016). "Impact of a Solar X-Flare on NVIS Propagation: Daytime characteristic wave refraction and nighttime scattering." IEEE antennas and propagation magazine 58.6: 29-37.

Web resources

Dst Index: https://www.aer.com/science-research/space/space-weather/space-weather-index/

SpaceX operation: https://www.space.com/solar-geomagnetic-storms-spacex-starlink-threat

SumbandilaSat Failure: https://www.defenceweb.co.za/joint/science-a-defence-technology/sumbandilasat-beyond-repair/

Appendix: Authors

Author	Affiliation
Pietro Vermicelli	Spacearth Technology Srl
Sara Mainella	Spacearth Technology Srl
Lucilla Alfonsi	Instituto Nazionale di Geofisica e Vulcanologia
Anna Belehaki	Institute for Astronomy, Astrophysics, Space Applications and Remote Sensing
Dalia Buresova	Institute of Atmospheric Physics of the Czech Academy of Sciences
Reko Hynönen	Sodankylä Geophysical Observatory
Vincenzo Romano	Instituto Nazionale di Geofisica e Vulcanologia
Ben Witvliet	University of Twente

CREDITS

Front cover image: Aurora over northern Canada

Page six: Solar Flare April 30, 2022,

Stay in touch with
PITHIA-NRF

CONTACTS

FIND US ON

PITHIA-NRF YouTube

in/pithia-nrf-research-infrastructure

@pithianrf

Project Homepage | www.pithia-nrf.eu
TNA | tna@pithia-nrf.eu
News Section | www.pithia-nrf.eu/news